Dengue Virus dependence on glucokinase activity and glycolysis Confers Sensitivity to NAD(H) biosynthesis inhibitors

Eva Ogire, Laure Perrin-Cocon, Marianne Figl, Cindy Kundlacz, Clémence Jacquemin, Sophie Hubert, Anne Aublin-Gex, Johan Toesca, Christophe Ramière, Pierre-Olivier Vidalain, et al.

▶ **To cite this version:**

Eva Ogire, Laure Perrin-Cocon, Marianne Figl, Cindy Kundlacz, Clémence Jacquemin, et al.. Dengue Virus dependence on glucokinase activity and glycolysis Confers Sensitivity to NAD(H) biosynthesis inhibitors. Antiviral Research, 2024, 228, pp.105939. 10.1016/j.antiviral.2024.105939 . hal-04743199

HAL Id: hal-04743199
https://hal.science/hal-04743199v1

Submitted on 18 Oct 2024

HAL is a multi-disciplinary open access archive for the deposit and dissemination of scientific research documents, whether they are published or not. The documents may come from teaching and research institutions in France or abroad, or from public or private research centers.

L'archive ouverte pluridisciplinaire **HAL**, est destinée au dépôt et à la diffusion de documents scientifiques de niveau recherche, publiés ou non, émanant des établissements d'enseignement et de recherche français ou étrangers, des laboratoires publics ou privés.

Distributed under a Creative Commons Attribution - NonCommercial - NoDerivatives 4.0 International License

Antiviral Research 228 (2024) 105939

Contents lists available at ScienceDirect

Antiviral Research

journal homepage: www.elsevier.com/locate/antiviral

Dengue Virus dependence on glucokinase activity and glycolysis Confers Sensitivity to NAD(H) biosynthesis inhibitors

Eva Ogire [a,2], Laure Perrin-Cocon [b,2], Marianne Figl [b,2], Cindy Kundlacz [b,1,2], Clémence Jacquemin [b], Sophie Hubert [b], Anne Aublin-Gex [b], Johan Toesca [b], Christophe Ramière [b,c], Pierre-Olivier Vidalain [b,3], Cyrille Mathieu [a,3], Vincent Lotteau [b,d,3], Olivier Diaz [b,*]

[a] CIRI, Centre International de Recherche en Infectiologie, NeuroInvasion TROpism and VIRal Encephalitis Team, Univ Lyon, Inserm, U1111, Université Claude Bernard Lyon 1, CNRS, UMR5308, ENS de Lyon, 21 Avenue Tony Garnier, F-69007, Lyon, France
[b] CIRI, Centre International de Recherche en Infectiologie, VIRal Infection Metabolism and Immunity Team, Univ Lyon, Inserm, U1111, Université Claude Bernard Lyon 1, CNRS, UMR5308, ENS de Lyon, 21 Avenue Tony Garnier, F-69007, Lyon, France
[c] Laboratoire de Virologie, Hôpital de la Croix-Rousse, Hospices Civils de Lyon, Lyon, France
[d] Laboratoire P4-Jean Mérieux, INSERM, Lyon, France

ARTICLE INFO

Keywords:
Dengue virus NS3
Glycolysis
Glucokinase regulator protein
NAD(H) metabolism
Hepatocyte
Primary organotypic liver cultures

ABSTRACT

Viruses have developed sophisticated strategies to control metabolic activity of infected cells in order to supply replication machinery with energy and metabolites. Dengue virus (DENV), a mosquito-borne flavivirus responsible for dengue fever, is no exception. Previous reports have documented DENV interactions with metabolic pathways and shown in particular that glycolysis is increased in DENV-infected cells. However, underlying molecular mechanisms are still poorly characterized and dependence of DENV on this pathway has not been investigated in details yet. Here, we identified an interaction between the non-structural protein 3 (NS3) of DENV and glucokinase regulator protein (GCKR), a host protein that inhibits the liver-specific hexokinase GCK. NS3 expression was found to increase glucose consumption and lactate secretion in hepatic cell line expressing GCK. Interestingly, we observed that GCKR interaction with GCK decreases DENV replication, indicating the dependence of DENV to GCK activity and supporting the role of NS3 as an inhibitor of GCKR function. Accordingly, in the same cells, DENV replication both induces and depends on glycolysis. By targeting NAD(H) biosynthesis with the antimetabolite 6-Amino-Nicotinamide (6-AN), we decreased cellular glycolytic activity and inhibited DENV replication in hepatic cells. Infection of primary organotypic liver cultures (OLiC) from hamsters was also inhibited by 6-AN. Altogether, our results show that DENV has evolved strategies to control glycolysis in the liver, which could account for hepatic dysfunctions associated to infection. Besides, our findings suggest that lowering intracellular availability of NAD(H) could be a valuable therapeutic strategy to control glycolysis and inhibit DENV replication in the liver.

1. Introduction

Viruses depend on host cell metabolism to acquire the energy and metabolites they need for their replication. They feed on cellular resources but in many cases, they have also evolved mechanisms to actively induce metabolic reprogramming to meet their needs, modulating the expression or activity of numerous metabolic enzymes (Sanchez and Lagunoff, 2015; Mayer et al., 2019; Thaker et al., 2019). Viruses interfere especially with central carbon metabolism (CCM (Diaz et al., 2022; Girdhar et al., 2021)) including glycolysis which produces both ATP and intermediate metabolites required for the biosynthesis of complex molecules. By characterizing the metabolic pathways

* Corresponding author.
E-mail address: olivier.diaz@inserm.fr (O. Diaz).
[1] Current address: Institute for Infectious Diseases, Faculty of Medicine, University of Bern, Bern, Switzerland.
[2] These authors contributed equally to this work.
[3] These authors contributed equally to this work.

https://doi.org/10.1016/j.antiviral.2024.105939
Received 1 February 2024; Received in revised form 20 May 2024; Accepted 17 June 2024
Available online 22 June 2024
0166-3542/© 2024 The Authors. Published by Elsevier B.V. This is an open access article under the CC BY license (http://creativecommons.org/licenses/by/4.0/).

modulated by viruses, these studies have identified key enzymatic cascades essential for viral replication. This provides basic knowledge on metabolic pathways and virus-host interactions. It has also led to the development of innovative therapeutic approaches based on the targeting of host cell metabolism to restrict viral growth (Erken et al., 2021).

Research carried out on different species of the *Flaviviridae* family, which includes major human pathogens such as hepatitis C virus (HCV), dengue virus (DENV), West Nile virus (WNV), Japanese encephalitis virus (JEV) and Zika virus (ZIKV), illustrates these "viro-metabolic" interactions. *Flaviviridae* are enveloped viruses with a single-stranded RNA genome of positive polarity encoding a large polyprotein that is processed by viral and cellular proteases into mature structural and non-structural (NS) proteins. Because HCV is associated with liver steatosis in chronically infected patients, this virus has been extensively studied for its ability to interfere with carbohydrate-lipid metabolism. At cellular level, HCV infection stimulates the synthesis of neutral lipids in hepatocytes, promoting the formation of replication complexes on the surface of cytosolic lipid droplets. Furthermore, HCV uses the lipoprotein synthesis pathway to produce low-density virions enriched in triglycerides (TG), called lipo-viral particles (LVP), which are essential for its propagation (Diaz et al., 2008, 2022; Piver et al., 2017; Scholtes et al., 2012). Several key proteins related to lipid metabolism were shown to be induced or activated by HCV, leading to increased lipogenesis and lipid accumulation in infected hepatocytes (Shimotohno, 2021; Dubuisson and Cosset, 2014). In addition, HCV infection has been associated with increased consumption of simple metabolites, notably glucose, to fuel lipogenesis and meet the needs for replication (Diamond et al., 2010; Ramière et al., 2014). Importantly, this ability to modulate lipid metabolism is not unique to HCV, but extends to mosquito-borne *Flaviviridae* that are responsible for acute infections such as ZIKV (Martín-Acebes et al., 2019), WNV (Martín-Acebes et al., 2014), JEV (Kao et al., 2015) and DENV (Heaton et al., 2010; Jordan and Randall, 2017). In the case of DENV, several studies showed that infection increases glycolysis and lipogenesis in infected cells (Jordan and Randall, 2016, 2017; Lee et al., 2020). An interaction was identified between the NS3 protein of DENV and fatty acid synthase (FASN) at the virus replication site (Heaton et al., 2010). This interaction was associated with higher fatty acid biosynthesis in DENV-infected cells, while *de novo* synthesized lipids preferentially co-fractionate with DENV RNA, suggesting a direct effect of the viral protein on enzymatic activity (Heaton et al., 2010). In addition, it has been shown that intracellular fatty acids become a source of energy via beta-oxidation for infected cells (Fernandes-Siqueira et al., 2018), illustrating the fine tuning of anabolic vs catabolic pathways by DENV.

In addition to lipids, *Flaviviridae* also increase the consumption of glucose which is a major source of metabolites and energy. However, the molecular mechanisms involved are still poorly characterized. Large-scale mapping of virus-host interactions provide valuable insights on cellular viral cycle (Perrin-Cocon et al., 2020; Hafirassou et al., 2017), and a few studies have identified some direct modulation of cellular enzyme activity by viral proteins (Ramière et al., 2014; Kao et al., 2015; Fontaine et al., 2014; Allonso et al., 2015; Perrin-Cocon et al., 2022). In particular, we have demonstrated that the NS5A protein of HCV interacts directly and increases the activity of hexokinases, which are the first rate-limiting enzymes of glycolysis that catalyze glucose phosphorylation to produce glucose-6-phosphate (G6P)(Ramière et al., 2014; Perrin-Cocon et al., 2022). This virus-host interaction increases glucose consumption and the level of triglyceride biosynthesis. For DENV, an interaction between NS3 and glyceraldehyde-3-phosphate dehydrogenase (GAPDH) was reported to decrease GAPDH glycolytic activity (Silva et al., 2019). Meanwhile, DENV infection increases glycolysis, which suggests the possible accumulation of glycolysis intermediates essential for the connected anabolic pathways (Lee et al., 2020; Fernandes-Siqueira et al., 2018; Fontaine et al., 2014), however underlying mechanisms remain unknown.

The human genome contains five genes encoding distinct hexokinase isoenzymes, known as HK1, HK2, HK3, GCK (for glucokinase) and HKDC1, with distinct enzyme properties and tissue distributions. GCK is mainly expressed in pancreas and liver, and is a monomeric allosteric enzyme with a higher Km for glucose compared to other hexokinases. Whereas GCK is inactive at normal blood glucose concentration, it becomes highly active when glucose availability rises, thus contributing to normalize glycemia. When necessary, to slow down cellular glycolysis, GCK activity is negatively regulated by the glucokinase regulator protein (GCKR) through direct interaction (Beck and Miller, 2013). In order to understand how DENV interferes with glycolysis in infected cells, we analyzed virus-host protein interactions and serendipitously found that NS3 interacts with GCKR. This observation is unsettling given that the prevalence of liver damage in dengue hemorrhagic fever is as high as 80% in some studies and hepatomegaly increases the risk of developing a severe form of dengue infection (Leowattana and Leowattana, 2021). Thus, although dengue infects different tissues, liver infection correlates with the severity of the disease. Hence, DENV-NS3 interaction with GCKR suggests a specific interference between DENV infection and regulation of GCK in the liver. We thus investigated how do DENV replication and NS3 viral protein interfere with glycolysis in hepatocytic cells. We demonstrated that GCKR modulation interfered with viral replication and that decreasing cellular glycolytic activity using 6-aminonicotinamide (6-AN), a pharmacological inhibitor of NADH metabolism, inhibited DENV replication. This antiviral effect was confirmed in primary organotypic liver cultures (OLiC) from hamsters, demonstrating that lowering intracellular availability of NADH is a potential therapeutic strategy to inhibit DENV replication in the liver.

2. Materials and methods

2.1. Cell culture and reagents

Unless otherwise stated, all chemicals were from Merck Sigma-Aldrich (Saint Quentin-Fallavier, France) and cell culture reagents were from Life Technologies (ThermoFisher Scientific, Saint Aubin, France).

2.2. Replicon

Plasmid containing the subgenomic replicon DENV-R2A or containing the full-length genome DENV-G2A were obtained from Ralf Bartenschlager (Department of Molecular Virology, Heidelberg, Germany). Plasmid pFK-DVs-R2A was linearized with XbaI (100 µL reaction): 10 µg plasmid DNA, 10 µL 10X buffer (50 mM Potassium Acetate, 20 mM Tris-acetate, 10 mM Magnesium Acetate, pH 7.9), 1 µL 100X BSA, 5 µL XbaI (20 U/µL), and H_2O to 100 µL. After 2 h incubation at 37 °C, the plasmid was purified using the NucleoSpin® Gel and PCR Clean-up kit (Macherey-Nagel, Hoerdt, France). RNA transcription was performed as previously described (Fischl et al., 2013). RNA was synthesized using the SP6 promoter using mMESSAGE mMACHINE^{tm} SP6 Transcription Kit (Ambion, ThermoFisher Scientific) and accordingly to provider recommendations. Viral RNA was purified from reaction mix using precipitation with lithium chloride and quantified by absorbance measurement. Purified RNA was immediately frozen at -80 °C until transfection. RNA was transfected into cells in suspension by electroporation as described (Fischl et al., 2013; Scholtes et al., 2008). Electroporation conditions were 960 µF and 270 V with a Gene Pulser system (Bio-Rad, Marnes-la-Coquette, France) in a cuvette with a gap width of 0.4 cm (Bio-Rad). Immediately after electroporation, cells were resuspended in complete medium and seeded in 96 wells plates. For assaying the luciferase activity, cells were washed once with PBS, and lysed directly in the plate by incubation during 20 min at room temperature with 50 µL of ice-cold Passive Lysis Buffer (Promega, Charbonnières-les-Bains, France). 30 µL of cell lysates were transferred to white 96 wells plates and 100 µL of Renilla-Glo® Luciferase Assay System mix

added before luminescence quantification using a luminometer Tristar 5 (Berthold, Freiburg, Germany) for 5 s. To normalize RNA electroporation efficiency, basal luminescence was measured at 4 h post-electroporation. Replication at latter times was expressed as fold of RLU at 4 h.

2.3. DENV infection

Virus stocks were obtained by transfecting BHK-21 cells with in vitro transcripts of the recombinant DENV genome containing the GFP (genotype 2, strain 16681) (Fischl et al., 2013). Infectivity titers in culture supernatants and virus stocks were quantified by determining the tissue culture infectious dose 50 (TCID50) per milliliter using a limiting dilution assay as described elsewhere (Lindenbach et al., 2005). Huh7 and Huh7-*GCK*$^{+}$/*HK2*$^{-}$ cells were seeded one day before infection at a MOI = 0.1. The day of infection, cells were washed twice before incubation with Opti-MEM™ I Reduced Serum Medium containing DENV for 4 h. Then, inoculum was removed and cells incubated with complete medium for the duration of the experiment.

2.4. Animals and ethical authorization

Syrian golden hamsters (Mesocricetus auratus) used in this study were obtained from Janvier Labs (Le Genest-Saint-Isle, France) with clean health monitoring report. The sex of the animals was random and dependent on the litter threw by the mother. Animals were euthanized at seven to nine days old. This study was performed according to French ethical committee (CECCAPP) regulations (accreditation CECCAPP_ENS_2014_034).

2.5. Preparation of Organotypic liver cultures (OLiC)

The procedure was adapted from the protocol for Organotypic Brain Cultures (OBC) described previously (Welsch et al., 2017). One day before the dissection, Millicell® cell culture inserts with PTFE membranes (Merck) were pre-activated with OLiC medium. The OLiC medium contains 375 mL of Minimal Essential Medium GlutaMAX (ThermoFisher Scientific), 125 mL of heat-inactivated horse serum (Gibco), 2.5 g of D-glucose (Sigma-Aldrich) and 1 mL of human recombinant insulin (10 mg/mL) (Sigma-Aldrich), and was sterilized with a 0.22 μm-pore size filter. The OLiC medium is identical to the OBC medium described elsewhere by Welsch et al. (2017) and used by Ferren et al. (2021) and Shyfrin et al. (2022) for organotypic brain, lung, and kidney cultures. Seven to nine-day suckling hamsters were sacrificed and their abdominal cavity was opened. Livers were collected and placed into a solution of Hibernate®-A medium (Sigma-Aldrich) supplemented with 100 I.U./mL of penicillin and 100 μg/mL streptomycin (Corning). The biggest lobe of the liver was isolated and was placed on 3 layers of Whatman paper with their longitudinal axis perpendicular to the tissue chopper blade and sliced transversely using the McIlwain® tissue chopper (Campden Instruments) at 500 μm thickness for all experiments. The slices were dissociated under a dissection microscope. Undamaged and homogenous slices were selected and maintained on an air-liquid interface provided by PTFE membranes pre-activated with OLiC medium.

2.6. OLiC infection

A 2 μL drop containing 1000 viral plaque-forming units (pfu) of the DENV2-EGFP was placed on each organotypic liver slice. Infected slices were incubated at 37 °C until collection. For treatment with 6-AN, the compound was diluted at the appropriate concentration in the culture medium (100 μM), and slices were then treated by adding a 2 μL drop of this medium on the top of each slice daily until the end of the experiment; For Mock treatments, OLiC were treated with medium containing DMSO at the equivalent concentration to 6-AN treated samples. Viral progression was followed by epifluorescence microscopy. Pictures were obtain using a Nikon Eclipse Ts2R optical microscope and stitched using the Stitching plugin in ImageJ. 90 h post-treatment, MTT assay was performed to evaluate the metabolic activity. 100 μL of 3-(4,5-dimethylthiazol-2-yl)-2,5-diphenyltetrazolium bromide were added per slice directly in insert and incubated 4 h at 37 °C. Slices were transferred in a plate (one slice per well) with 200 μL of DMSO and heated 10 min at 37 °C to solubilize formazan. 75 μL of these were transferred and the absorbance was measured at OD = 490 nm and OD 570 nm (Tristar 5, Berthold).

2.7. ORF cloning into gateway-compatible plasmids

NS3 full length, NS3 helicase or NS3 protease ORFs were cloned from DENV genotype 2 (strain 16,681), using the Gateway recombination-based cloning system (de Chassey et al., 2008). Viral ORFs were PCR-amplified (with Novagen KOD polymerase, Merck-Millipore) from a DNA template using sequence-specific primers fused to attB1.1 and attB2.1 recombination sites. PCR products were subsequently cloned into pDONR223 to generate entry plasmids (BP Clonase II Enzyme mix; ThermoFisher Scientific). Entry plasmid containing the ORF of GCKR was picked from the Human ORFeome v3.1 collection (Open Biosystem, Huntsville, AL, USA (Lamesch et al., 2007)). Each ORF was transferred by in vitro recombination into the different Gateway-compatible destination vectors used in this study (LR Clonase II Enzyme mix; Life Technologies). LR reaction products were subsequently transformed into DH5α competent bacterial cells and grown overnight on LB-agarose plates containing ampicillin before amplification into liquid LB medium also containing ampicillin. Plasmids were purified using a NucleoSpin Plasmid kit from Macherey-Nagel and validated by sequencing (Eurofins, Nantes, France).

2.8. Glucose and lactate quantification

Metabolites were quantified from cell supernatants using the Glucose Oxidase (GO) assay kit and the Lactate assay kit from Millipore Sigma-Aldrich. Assays were performed according to the manufacturer's instructions and results were normalized to protein quantity (DC Protein Assay; Bio-Rad) or number of cells per sample.

2.9. Reverse transcription-quantitative PCR (RT-qPCR)

Total RNA from tissue slices was extracted using the NucleoSpin RNA extraction kit (Macherey-Nagel) according to manufacturer instructions. Viral RNA was extracted from culture supernatant using the QIAmp viral RNA extraction kit with AVL Buffer (Qiagen, Les Ulis, France) according to manufacturer instructions. cDNA was obtained by reverse transcription of 250 ng of the extracted RNA using High-Capacity cDNA Reverse Transcription kit (Applied Biosystems, Thermo Fisher Scientific) according to manufacturer protocol, in a final reaction volume of 20 μL. 0.4 μL of the cDNA reaction product was used for qPCR using QuantiNova SYBR Green RT-PCR Master Mix (Qiagen) in the presence of 0.5 μM of the following primers: 5′- GAGCGTGAAAAGGTGGATGC-3′ and 5′-TGTCTGCGTAGTTGATGCCTT-3′ for DENV cDNA amplification, 5′-AAAAGCGGATGGTGGTTCCT-3′ and 5′-GCTGTCACTGCCTGGTACTT-3′ for RLP13a cDNA amplification. PCR was performed with the StepOnePlus Quantitative PCR System (Applied Biosystems, ThermoFisher Scientific) and analyzed with the StepOne v2.3 software (Applied Biosystems).

2.10. Protein-complementation assay (PCA)

NS3 interaction with GCKR was determined by NanoLuc Two-Hybrid (N2H) assay, a recently developed split-luciferase complementation assay (Choi et al., 2019). In this system, two complementary fragments of NanoLuc, F1 and F2, are fused to proteins of interest. The

reconstitution of NanoLuc activity by trans-complementation of F1 with F2 is dependent on the physical interaction of candidate proteins. This assay was used to test the interaction of GCKR with either NS3 full-length or its helicase or its protease domains. The NS3 coding sequences were cloned by in vitro recombination (Gateway system; Thermo Fisher) from entry plasmids into pDEST-N2H–N1, whereas the GCKR sequence was cloned into the pDEST-N2H–C2 vector. The obtained constructs were co-transfected in HEK-293T cells with the Jet-Prime reagent (Polyplus-Transfection, Illkirch-Graffenstaden, France). This allowed for the co-expression of NS3 N-terminally tagged with fragment F1 of NanoLuc together with GCKR C-terminally tagged with fragment F2 of NanoLuc. After 48 h of culture, cells were lysed and NanoLuc activity was determined as previously described (Coutant et al., 2019; Giraud et al., 2021). The bioluminescent signal obtained when co-expressing N1-NS3 and GCKR-C2 was compared to the sum of the signals obtained when co-expressing N1-NS3 with F2 or GCKR-C2 with F1 (background signal).

2.11. Western-blot analysis

Cell lysates were prepared in lysis buffer (1% Triton X-100, 5 mM EDTA in PBS with 1% protease inhibitor cocktail (Merck Sigma-Aldrich)). After elimination of insoluble material, proteins were quantified, separated by SDS-PAGE and analyzed by western-blot on PVDF membrane. After saturation of the PVDF membrane with PBS-0.1% Tween 20 supplemented with 5% (w/v) non-fat milk powder, blots were incubated 1 h at room temperature with the primary antibody in PBS-0.1% Tween 20 (1:2000 dilution). After washing, incubation with the secondary HRP-labeled antibody (1:10,000 dilution) was performed for 1 h at room temperature and detected by enhanced chemiluminescence reagents according to the manufacturer's instructions (SuperSignal Chemiluminescent Substrate, Thermo Fisher Scientific).

2.12. Statistics and reproducibility

All statistical analyses were performed with GraphPad Prism software. The confidence interval was set to 95% in all statistical tests. Details of statistical analyses can be found in the figure legends. The *p* values and sample size (n) are indicated either directly in the figure or in the legend. The mean ± standard error of the mean (SEM) is displayed unless otherwise stated.

3. Results

3.1. DENV-NS3 protein interacts with GCKR and enhances glycolysis

DENV-NS3 protein was previously reported to bind GAPDH and inhibit its activity (Silva et al., 2019), potentially enabling the accumulation of glycolysis intermediates essential for connected anabolic pathways. As part of a prospective study to identify new protein-protein interactions (PPIs) between viral factors and cellular enzymes of the glycolytic pathway, we found that the NS3 protein of DENV binds GCKR, the negative regulator of GCK. This was achieved by NanoLuc Two-Hybrid (N2H) technology, a split-luciferase complementation assay, developed for PPIs detection (Choi et al., 2019). Two complementary fragments of the bioluminescent enzyme NanoLuc were fused to GCKR and DENV-NS3, respectively. Once the two constructs were co-expressed in HEK-293T cells, the luciferase activity which depends on

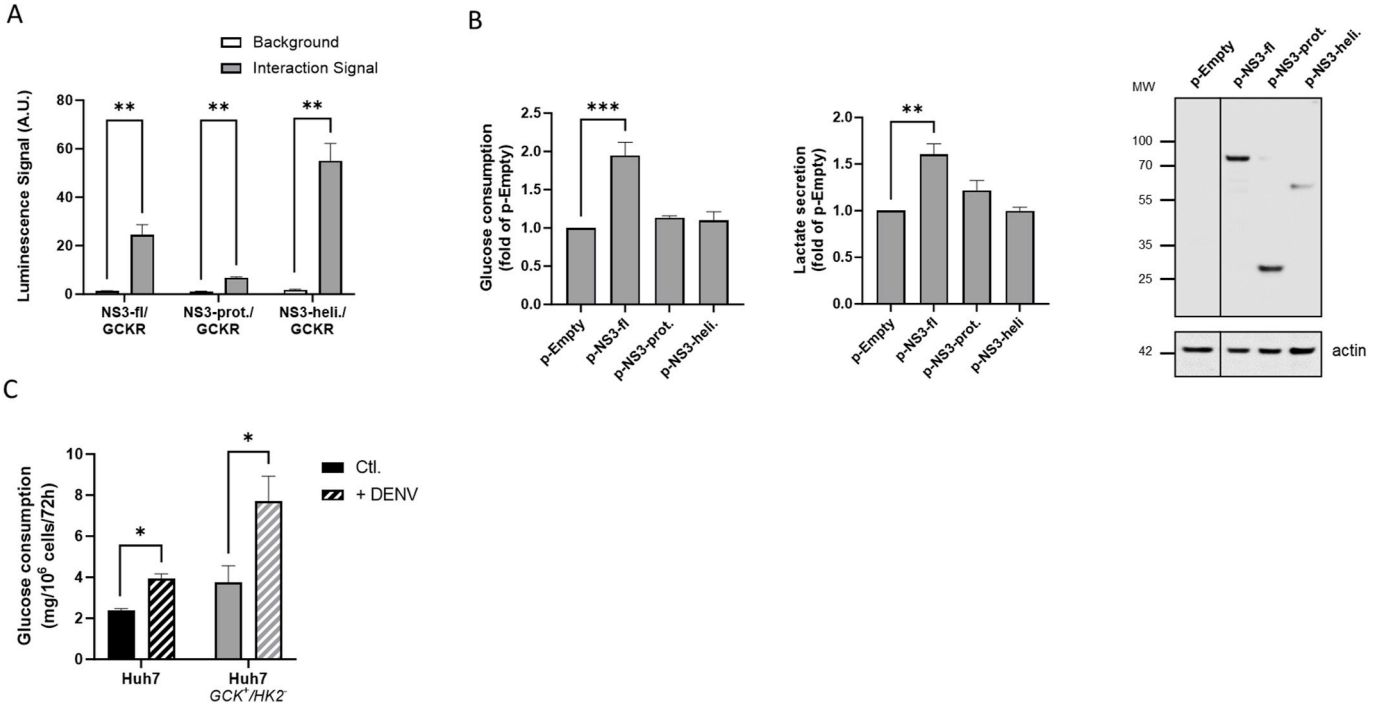

Fig. 1. DENV-NS3 interacts with GCKR and induces glycolysis. A) Data showing the luminescence signal resulting from interaction of DENV-NS3 full length (NS3-fl), DENV-NS3 protease (NS3-prot.) or DENV-NS3 helicase (NS3-heli.) with GCKR (grey bars). See material and methods for experimental details. Background luminescence of non-specific interaction was determined in each experiment and presented (white bars). Data presented means ± SEM (n = 3) and *p* values were determined by two-way ANOVA for multiple comparison (** $p < 0.01$). **B)** Glucose consumption and lactate secretion were determined in 48 h cultures of Huh7-*GCK*$^{+}$/*HK2*$^{-}$ cells transfected with plasmids 3xFlag coding or not for NS3-full length, NS3-protease or -helicase domains. Data are normalized to control condition transfected with the empty plasmid. Data presented means ± SEM (n = 3) and *p*-values were determined by one-way ANOVA for multiple comparison (** $p < 0.01$). Western-blot showing the expression of DENV-NS3 full length or its domains. 30 μg of whole protein lysate were loaded on the gel for each condition and blotting was revealed with anti-3Flag or anti-actin antibody. **C)** Glucose consumption in cell supernatant of mock or sgDENV-R2A electroporated Huh7 and Huh7-*GCK*$^{+}$/*HK2*$^{-}$ cells, after 72 h of culture. Cells were harvested and counted to normalize glucose consumption. Presented data correspond to 3 experiments, and *p*-values were determined by two-way ANOVA for multiple comparison (* $p < 0.05$).

reconstitution of the NanoLuc enzyme, demonstrated an interaction between NS3 and GCKR (Fig. 1A). Although full-length NS3 (NS3-fl) or its isolated protease domain (NS3-prot) showed an interaction with GCKR, the strongest signal was observed with the helicase domain of NS3 (NS3-heli) suggesting that this region plays a preponderant role in the interaction with GCKR.

Since GCKR is an important regulator of GCK hexokinase activity in the liver, we investigated the effect of NS3 expression on glycolysis in Huh7-*GCK*$^+$/*HK2*$^-$ hepatocytic cells. This cell line was previously described in details and corresponds to the hepatocellular carcinoma cell line Huh7 where the cancer-associated hexokinase HK2 was knocked-out and replaced by GCK, the isoenzyme expressed in primary hepatocytes (Perrin-Cocon et al., 2021). As opposed to parental Huh7, these cells respond to extracellular glucose concentrations and produce lipids similarly to primary hepatocytes. As shown in Fig. 1B, NS3-fl expression increased both glucose consumption and lactate secretion in Huh7-*GCK*$^+$/*HK2*$^-$ cells, indicative of an increase in glycolytic activity. In contrast, the isolated protease or helicase domains of NS3 had no effect, thus demonstrating that full length NS3 protein is required for a functional effect on glycolysis. Finally, we observed that replication of the subgenomic DENV replicon (sgDENV-R2A), expressing luciferase as a reporter instead of structural proteins (Chatel-Chaix et al., 2016), in Huh7-*GCK*$^+$/*HK2*$^-$ cells increased by 2-fold glucose consumption (Fig. 1C), which is in agreement with previous observations in human foreskin fibroblasts (Fontaine et al., 2014). Overall, these results shed light on how DENV-NS3 modulates glycolytic activity in infected liver cells, potentially by interfering with GCKR activity.

3.2. DENV replication depends on cellular hexokinase activity

Results presented above show that glycolysis is a pathway tightly regulated by DENV, suggesting that glucose is essential for viral replication. Whether glucose can be substituted by other sources of carbon is unknown. To address this question, we first analyzed DENV replication in Huh7-*GCK*$^+$/*HK2*$^-$ cultured in the presence of glucose or other sources of carbon such as glutamine or galactose, another hepatocyte-metabolizable hexose. As shown in Fig. 2A, the highest replication of DENV subgenomic replicon was observed with glucose. Neither supplementation with glutamine, galactose or both of them enabled strong DENV replication (Fig. 2A), whereas cell proliferation was not significantly different according to carbon source (Supplementary Fig. 1). Moreover, viral replication was proportional to glucose concentration in the culture medium up to 2 g/L (Fig. 2B). DENV replication thus depended particularly on the presence of glucose in cell culture medium which is fueling glycolysis.

To further support this conclusion, we compared the replication in Huh7-*GCK*$^+$/*HK2*$^-$ vs Huh7 cells expressing HK2. Indeed, we previously found that Huh7-*GCK*$^+$/*HK2*$^-$ cells had a higher glycolytic activity than Huh7 cells from which they are derived, with restored lipogenesis and glycogenesis (Perrin-Cocon et al., 2021). A recombinant strain of DENV type 2 expressing GFP as a viral growth reporter was used (DENV-GFP; strain 16681). Interestingly, we observed an increased infection of GCK-expressing cells compared to Huh7 cells expressing HK2 (Fig. 3A and B). Accordingly, replication of a DENV-R2A replicon was enhanced in transfected Huh7-*GCK*$^+$/*HK2*$^-$ cells compared to Huh7 cells (Fig. 3C and D) and confirmed by quantifying NS3 protein expression by western-blot (Fig. 3E). Therefore, Huh7-*GCK*$^+$/*HK2*$^-$ cells better replicate DENV than parental Huh7 cells expressing HK2.

To further establish the role of GCK in DENV replication, standard Huh7 cells were transduced with increasing amounts of a lentiviral vector expressing GCK. We observed that viral replication was proportional to the amount of GCK expressed in the cells (Fig. 4A and B), and correlated with hexokinase activity measured in homogenates of transduced cells (Fig. 4C). Taken together, these observations confirm that DENV depends on glucose for its replication, and that the level of GCK controls the level of viral replication.

3.3. DENV replication is repressed by GCKR expression in Huh7-*GCK*$^+$/*HK2*$^-$ cells

As mentioned above, GCKR is the natural repressor of GCK. In a feedback loop slowing down cellular glycolysis, fructose-6-phosphate acts as an allosteric effector of the interaction of GCKR with GCK, forcing GCK into a weakly active form (Beck and Miller, 2013). Since DENV replication depends on glycolysis, we tested whether modulation of GCK-GCKR interaction was able to control viral replication. We observed that the addition of fructose-6-phosphate at the moment of cell electroporation with DENV replicon, inhibited by about 50% viral replication (Fig. 5A). Conversely, addition in the cell culture medium of a GCK-GCKR interaction inhibitor (AMG-3969) increased DENV replication (Fig. 5B), further supporting the idea that GCK-GCKR interaction modulates viral replication. To confirm these observations, GCKR was overexpressed in order to limit GCK activity in Huh7-*GCK*$^+$/*HK2*$^-$ cells, resulting in reduced DENV replication (Fig. 5C). Mutations that impact

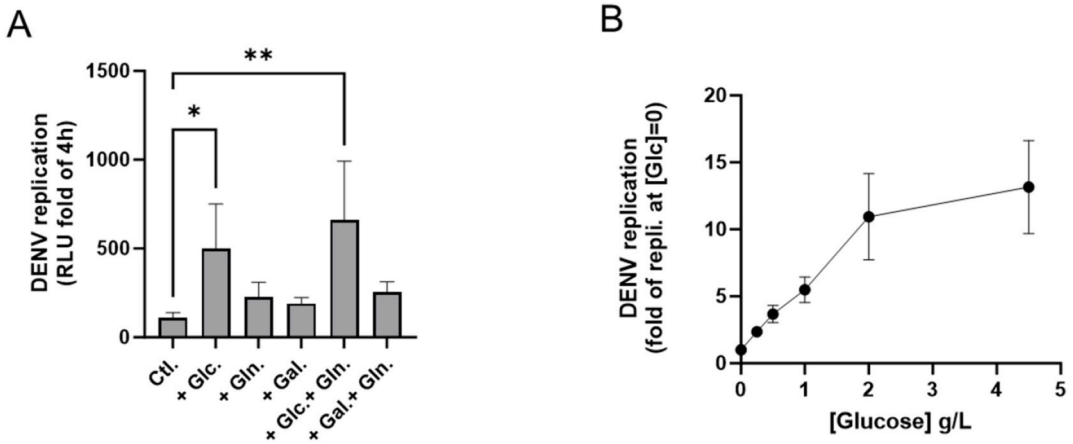

Fig. 2. Replication of DENV depends on glucose. A) Huh7-*GCK*$^+$/*HK2*$^-$ cells were electroporated with sgDENV-R2A replicon and cultured in DMEM medium containing SVF and pyruvate, in absence (Ctl.) or presence of glucose (+Glc.), or glutamine (+Gln.), or galactose (+Gal.) as indicated. 72 h post electroporation, Renilla luminescence was measured and normalized to the 4 h value that reflects transfection efficiency. Presented data correspond to means ± SEM of 3 experiments, and *p*-values were determined by one-way ANOVA for multiple comparison (* $p < 0.05$) **B)** Huh7-*GCK*$^+$/*HK2*$^-$ cells were electroporated with sgDENV-R2A replicon and cultured in presence of increasing concentration of glucose as indicated on the graph. Replication was determined after 72 h as in A) and normalized to replication at [Glucose] = 0. Presented data correspond to means ± SEM of 2 experiments.

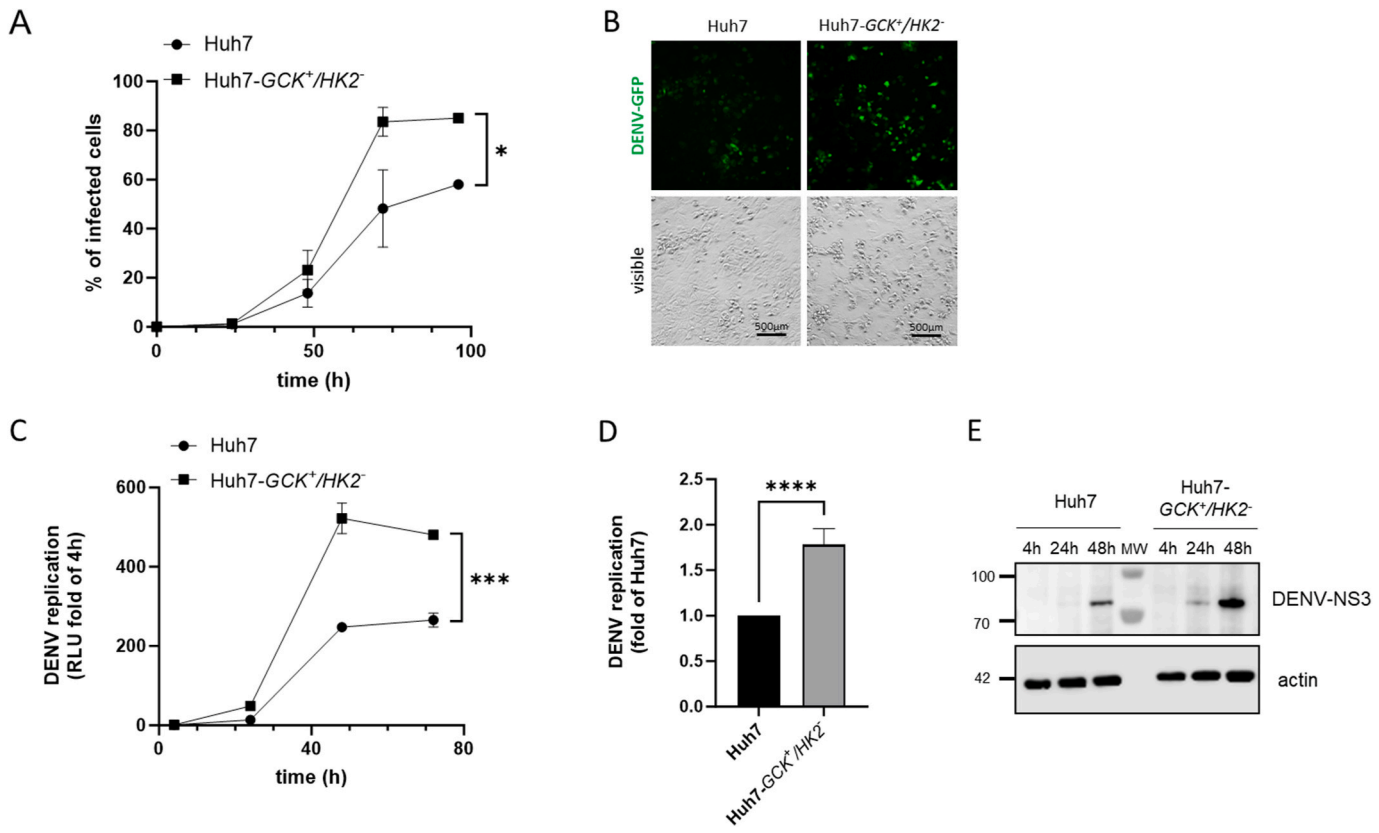

Fig. 3. Huh7-*GCK*$^{+}$*/HK2*$^{-}$ cells better replicate DENV than parental Huh7 cells. A) Cells were infected at a MOI = 0.1 with DENV-GFP and the percentage of infected cells was analyzed by flow cytometry at 24, 48, 72 and 96 h post-infection. Presented data correspond to means ± SEM of 3 experiments (* $p < 0.05$ was determined by two-way ANOVA). **B)** Observation by fluorescence and bright-field microscopy of infected cells at 72 h post infection. **C)** Cells were electroporated with sgDENV-R2A replicon and Renilla luminescence was analyzed at 4, 24, 48 and 72 h post-electroporation. Data were normalized to the 4 h value that reflects transfection efficiency. Presented data correspond to means ± SEM of 3 experiments. D) Replication of sgDENV-R2A at 72 h post-electroporation. Luciferase activity in cell lysates was normalized to Huh7 cells (n = 52, paired *t*-test, **** $p < 0.0001$). **E)** Western-blot of DENV-NS3 protein in cell homogenates after electroporation of sg-DENV-R2A replicon of one experiment. Actine was used as housekeeping gene.

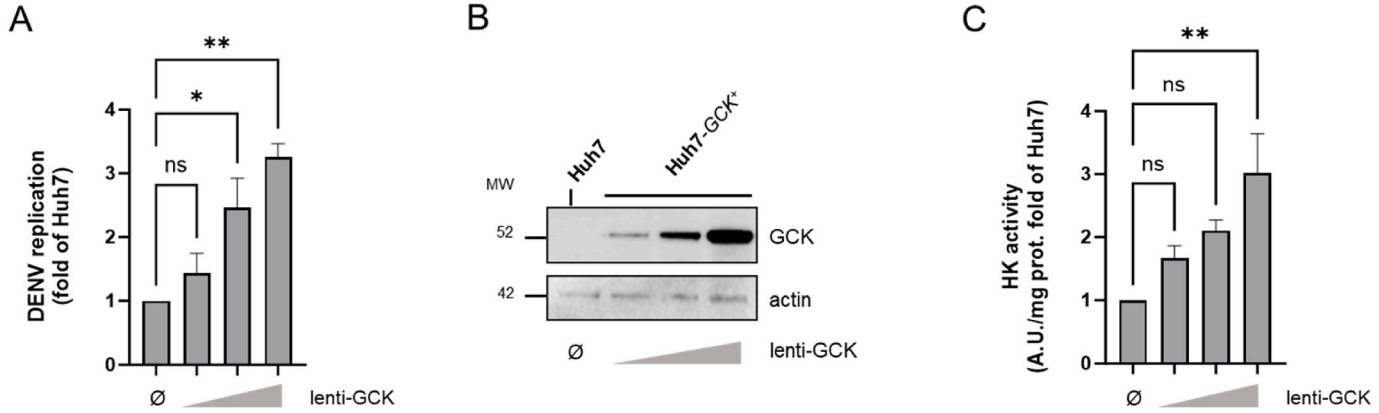

Fig. 4. DENV replication depends on GCK expression and activity. A) Huh7 cells were transduced with increasing amounts of a lentiviral vector expressing GCK as described in the Material and Methods section. Cells were electroporated with sgDENV-R2A replicon and Renilla luminescence analyzed at 72 h post-electroporation. Data were normalized to replication observed in mock-transduced Huh7 cells (Ø). Presented data correspond to means ± SEM of 3 experiments (* $p < 0.05$, ** $p < 0.01$, one-way ANOVA for multiple comparison). **B)** Western-blot showing the expression of GCK after lentiviral transduction. 30 µg of whole cellular protein lysate were loaded on the gel for each condition and blotting was revealed with anti-GCK or anti-actin antibody. **C)** Hexokinase activity determined in cell homogenates from cell lines obtained in A) and B). Presented data correspond to means ± SEM of 3 experiments (** $p < 0.01$, one-way ANOVA for multiple comparison).

GCKR's capacity to interact with GCK have been described in the literature. In particular, mutation D413A in GCKR, was reported to decrease its capacity to inhibit GCK (Choi et al., 2013). As expected, overexpression of the GCKR^{D413A} mutant in Huh7-*GCK*$^{+}$*/HK2*$^{-}$ cells had no effect on DENV replication (Fig. 5C). Interestingly, overexpression of wild-type GCKR or its mutant GCKR^{D413A} had no effect on DENV replication in Huh7 cells that do not express GCK (Fig. 5D), confirming that it is the specific inhibition of GCK by GCKR that inhibits viral replication.

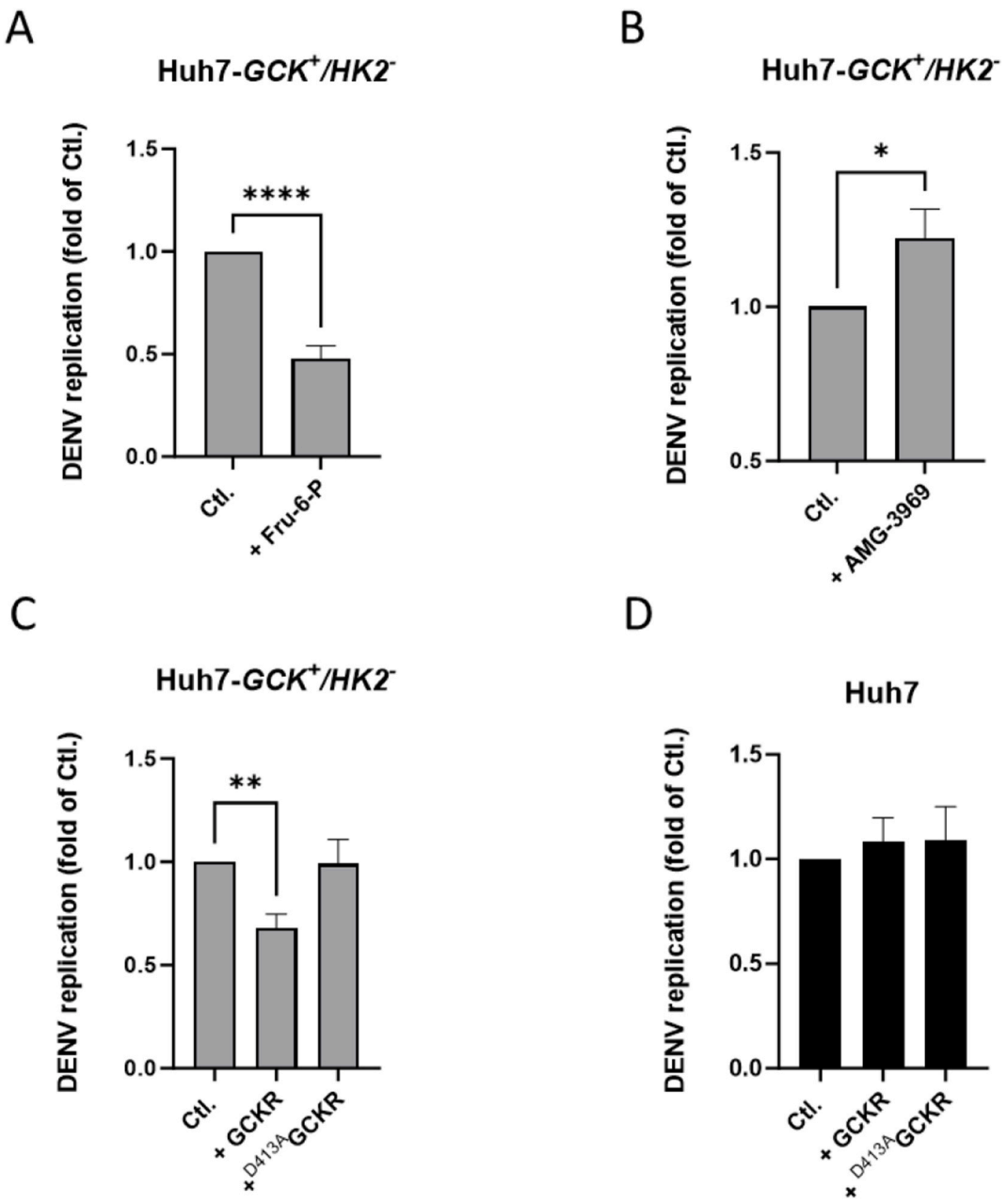

Fig. 5. GCKR modulates DENV replication in Huh7-*GCK*$^{+}$/*HK2*$^{-}$ cells. A) Huh7-*GCK*$^{+}$/*HK2*$^{-}$ cells were electroporated with sgDENV-R2A replicon in absence (Ctl.) or presence of 5 mM fructose-6-phosphate (+Fru-6-P) and Renilla luminescence was analyzed at 72 h post-electroporation. Luminescence was normalized to the 4 h value that reflects transfection efficiency. Replication was normalized to control. Presented data correspond to means ± SEM (n = 6, paired *t*-test, **** $p < 0.0001$). **B)** Huh7-*GCK*$^{+}$/*HK2*$^{-}$ cells were electroporated with sgDENV-R2A replicon and incubated in absence or presence of 1 μM AMG-3969 for 72 h. Renilla luminescence was analyzed and normalized to the 4 h value that reflects transfection efficiency. Replication was normalized to control (Ctl.). Presented data correspond to means ± SEM (n = 3, paired *t*-test, * $p < 0.05$). **C)** Huh7-*GCK*$^{+}$/*HK2*$^{-}$ cells or **D)** Huh7 cells were electroporated with sgDENV-R2A replicon and plasmid for GCKR or ^{D413A}GCKR expression. Renilla luminescence was analyzed at 72 h post-electroporation and luminescence was normalized to the 4 h value that reflects transfection efficiency. Replication was normalized to control (Ctl.). Presented data correspond to means ± SEM (n = 7, paired *t*-test, ** $p < 0.005$).

3.4. DENV replication is repressed by NAD synthesis inhibitor 6-amino-nicotinamide (6-AN)

NAD^{+} is essential for glycolysis as it is used by GAPDH and lactate dehydrogenase (LDH) as a coenzyme. 6-Aminonicotinamide (6-AN) is an inhibitor of NAD^{+} biosynthesis that affects several metabolic pathways including glycolysis and pentose phosphate pathway (PPP), as depicted in Fig. 6A. Since DENV-NS3 interferes with GCKR activity, the potential increase of G6P (product of glucose phosphorylation by hexokinases), could feed PPP to enhance the production of ribose-5-phosphate (R5P; Fig. 6A), a key precursor in the synthesis of purine and pyrimidine nucleotides. 6-AN is well known as a potent inhibitor of G6PD, which is the first enzyme controlling the entry of G6P into the PPP and the production of R5P. We thus tested the effect of 6-AN on DENV replication in Huh7-*GCK*$^{+}$/*HK2*$^{-}$ cells. As shown in Fig. 6B, DENV replication was suppressed by 80% in the presence of 6-AN. Surprisingly, this inhibition was not reverted by D-ribose (Fig. 6B), which can be phosphorylated by the ribokinase RBKS into R5P to sustain nucleotide biosynthesis (Sahoo et al., 2023; Pauly and Pepine, 2000). This suggested that inhibition of the PPP was not at the origin of DENV inhibition by 6-AN despite DENV's high dependence for nucleotides biosynthesis pathways in this model (see Fig. 6C showing that DENV replication is strongly suppressed

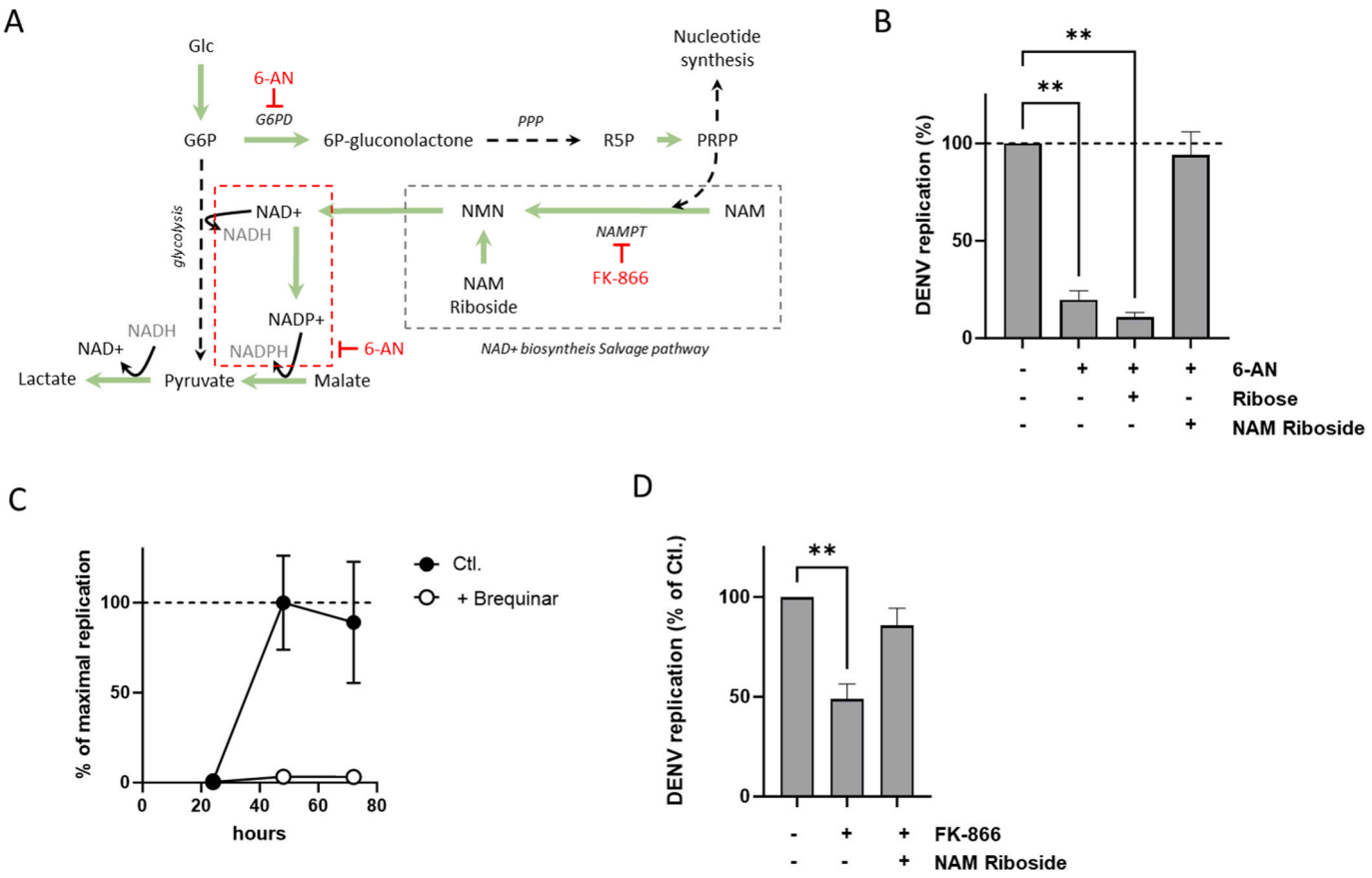

Fig. 6. Inhibition of NAD metabolism inhibits DENV replication. A) Schematic representation of glycolysis, connections with pentose-phosphate pathway (PPP) and NAD^+ biosynthesis salvage pathway and impact of drugs used in the present study (wrote in red). **B)** Huh7-*GCK*$^+$/*HK2*$^-$ cells were electroporated with sgDENV-R2A replicon and incubated in absence or presence of 0.5 mM 6-AN and/or 25 mM ribose and/or 0.5 mM NAM Riboside as indicated on graph, for 72 h. Renilla luminescence was analyzed and normalized to the 4 h value that reflects transfection efficiency. Replication was expressed as % of the replication in absence of treatment. Presented data correspond to means ± SEM (n = 3, ANOVA, ** $p < 0.01$). **C)** Huh7-*GCK*$^+$/*HK2*$^-$ cells were electroporated with sgDENV-R2A replicon and incubated in absence or presence of 1 μM Brequinar. Renilla luminescence was analyzed at 24, 48 and 72 h post-electroporation and normalized to the 4 h value. Replication was expressed as % of the maximal replication in control condition (Ctl.). Are presented means ± SEM of 3 experiments. **D)** Huh7-*GCK*$^+$/*HK2*$^-$ cells were electroporated with sgDENV-R2A replicon and incubated in absence or presence of FK-866 ± 0.5 mM NAM riboside for 72h. Renilla luminescence was analyzed and normalized to the 4 h value that reflects transfection efficiency. Replication was expressed as % of control (Ctl.). Are presented means ± SEM (n = 3, ANOVA, ** $p < 0.01$).

by pyrimidine biosynthesis inhibitor Brequinar).

In contrast, DENV replication inhibition by 6-AN was reverted by NAM riboside, a precursor of the NAD salvage pathway (Fig. 6B and Supplementary Fig. 2). Once internalized, 6-AN is used instead of nicotinamide (NAM) by nicotinamide phosphoribosyl transferase (NAMPT), the first enzyme of the Nicotinamide Adenine Dinucleotide (NAD) salvage pathway. It is thus metabolized into 6-Amino-Nicotinamide Adenine Dinucleotide (6ANAD) and 6ANAD Phosphate (6ANADP), which are non-reducible forms of NAD and NADP and thus inhibitors of enzymes using these metabolites as cofactors. We confirmed that DENV replication was indeed dependent on the activity of the NAD-salvage pathway, using the specific NAMPT inhibitor FK-866, whose effect was also reverted by the addition of NAM-riboside in the culture medium (Fig. 6D). This suggests that 6-AN metabolization into 6ANAD(P) decreases the pool of NAD(P) that is available for metabolic functions, in particular glycolytic NAD-dependent enzymes (Fig. 6A, dashed red line).

This was confirmed in Huh7-*GCK*$^+$/*HK2*$^-$ cells treated with 6-AN where a decrease in NAD^+ correlated with a lower consumption of glucose and addition of NAM riboside restored both the pool of NAD^+ and the consumption of glucose (Fig. 7A and B). As a consequence, intracellular ATP is decreased by 6-AN and restored by NAM riboside, revealing its indirect impact on CCM (Fig. 7C). At the same time, cell viability determined by trypan blue exclusion assay was not impacted by 6-AN treatment and cellular growth only weakly affected (Fig. 7D and E). It was further confirmed by the positive correlation between viral replication and intracellular ATP levels which are progressively restored by increasing doses of NAM riboside in presence of 6-AN (Supplementary Figs. 2 and 3). Overall, these observations indicate that inhibition of NAD biosynthesis by 6-AN is efficient to block glycolysis and inhibit DENV replication in cell cultures.

3.5. 6-An inhibits DENV replication in hamster-derived organotypic liver cultures

In this study, we used the Huh7-*GCK*$^+$/*HK2*$^-$ cell line, which is quite unique in that it enables analysis of both GCK and GCKR activities. However, it is important to note that although these cells express GCK instead of HK2, they remain cancer cells with an anabolism-oriented metabolism associated with high proliferation, unlike primary hepatocytes that do not proliferate. Therefore, we wondered whether 6-AN efficiently inhibited DENV replication in primary liver cells, *ex-vivo*. To answer this question, we infected hamster liver slices maintained in culture (OLiC) as previously performed for measles virus and SARS-CoV-2 infection of organotypic brain, lung and kidney cultures (Welsch et al., 2017; Ferren et al., 2021; Shyfrin et al., 2022). 500 μm-thick liver slices

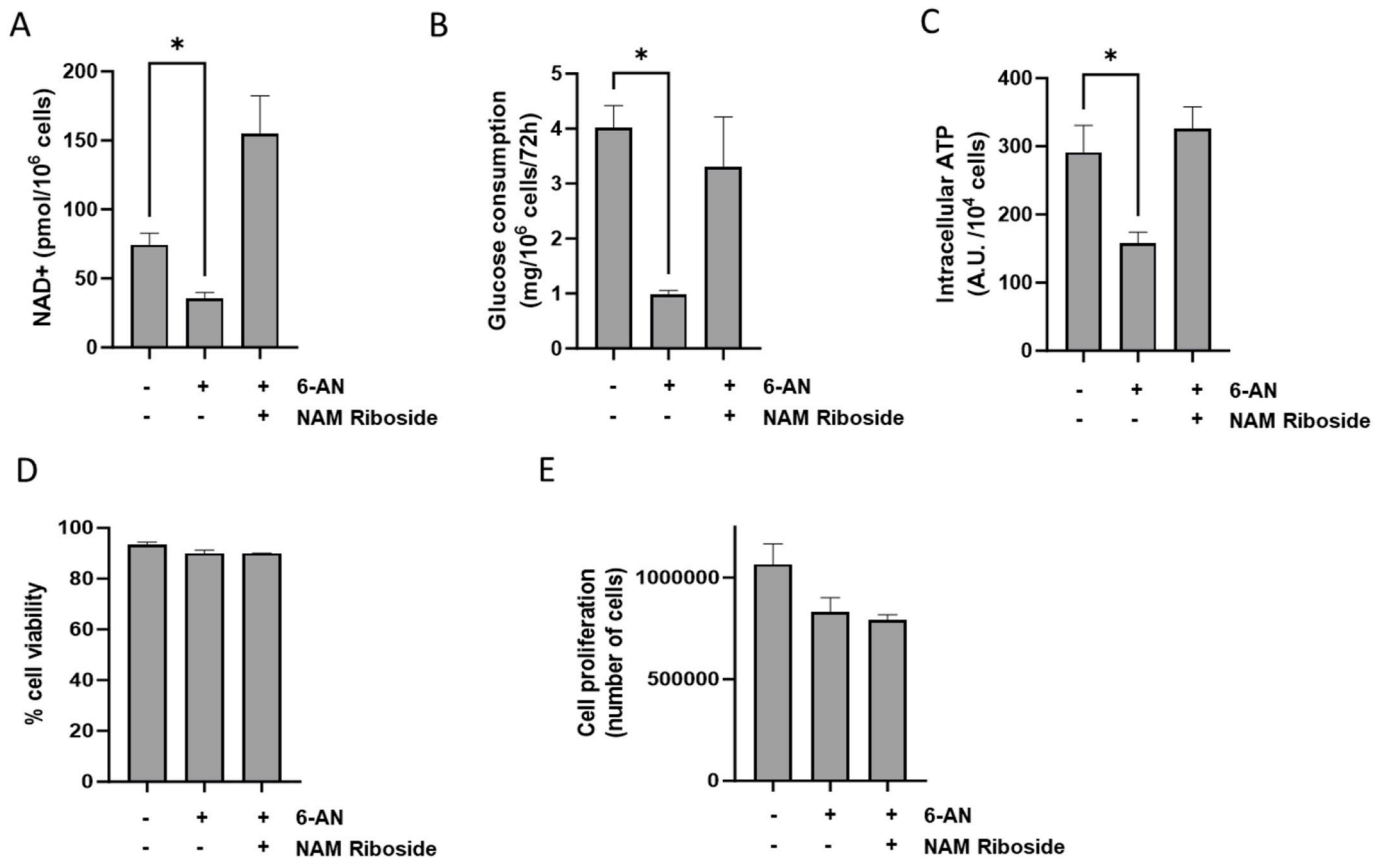

Fig. 7. Effect of 6-AN on cell metabolism. Huh7-*GCK*$^{+}$/*HK2*$^{-}$ cells treated or not with 0.5 mM 6-AN ± 0.5 mM NAM riboside for 72 h. **A)** NAD^{+} was quantified as indicated in material and methods in cells. **B)** Glucose consumption was determined in culture supernatant and **C)** intracellular ATP determined using luminescent assay. Are presented means ± SEM (n = 3, paired *t*-test * $p < 0.05$). **D)** % of viability and **E)** cell proliferation were determined after 72 h of culture. Are presented means ± SEM of 3 experiments.

from hamsters were cultured at the air/liquid interface on porous polytetrafluoroethylene (PTFE) membranes as described in Material and Methods. The day of slicing, OLiCs were infected with 10^3 PFU of DENV-GFP and treated or not with 100 μM 6-AN in the subnatant culture medium. 90 h post-infection, we were able to observe infectious GFP foci in liver slices cultured in control condition, whereas no infection was detected in liver slices treated by 6-AN (Fig. 8A). Total cellular RNA was extracted from liver slices and DENV genomes were quantified. We observed a 2 $\log_{10}$ decrease of intra-liver DENV genomes in presence of 6-AN (Fig. 8B) and a total inhibition of DENV particle secretion in culture medium (Fig. 8C). Quantification of ribosomal protein L13a (RPL13a) as a housekeeping gene revealed that 6-AN treatment had no impact on the quantity of extracted RNA (Fig. 8D and Supplementary Fig. 4A). 6-AN treatment had no impact as well on global metabolic activity determined by MTT assay (Fig. 8E and Supplementary Fig. 4B). Sodium Dodecyl Sulfate (SDS) was used in these experiments as a chemical inducer of cell death as already described for 3D cell culture models (Welch et al., 2021; Tseng et al., 2015). Indeed, SDS profoundly impacted tissue viability measured by MTT assay (Fig. 8E and Supplementary Fig. 4B) and completely annihilated quantity of extracted RNA (Supplementary Fig. 4A). These results indicate the absence of toxicity of 6-AN in OLiC. Altogether, these results confirm that 6-AN effectively inhibits DENV replication in primary liver cells.

4. Discussion

Studies analyzing how viruses control cellular metabolism to replicate have often overlooked the unique metabolic characteristics of the cell types they infect. Aside canonical hepatitis viruses A to E that mostly (or exclusively) replicate in the liver, several other viruses, including yellow fever virus in the first place, have a significant tropism for this organ (Mrzljak et al., 2019). This could relate to the unique metabolic functions of hepatocytes which play a pivotal role in the regulation of systemic metabolism. Since hepatocytes are a major source of various metabolites, it is not surprising that viruses targeting these cells have evolved dedicated strategies for manipulating the metabolism of these cells. Although DENV can replicate in many cell types, several studies have found the virus in the liver of deceased patients and shown its ability to replicate in primary human hepatocytes (Suksanpaisan et al., 2007; Aye et al., 2014). From a pathophysiological point of view, liver damage is a component of the natural history of the disease. Hepatomegaly is encountered in 10–80% of cases, depending on the study, and elevation of hepatitis markers such as AST is observed in 80–90% of cases (Leowattana and Leowattana, 2021). Hepatic steatosis was observed in patients in some studies (Aye et al., 2014). Even if we cannot exclude inflammation as a contributor to this symptom, the ability of the virus to directly induce and deregulate hepatocyte carbohydrate and lipid metabolism appears as a potential enhancer of clinical manifestations. Acute liver failure is also observed in some critical cases, ultimately leading to patient's death (Leowattana and Leowattana, 2021). It is therefore important to control DENV replication in the liver to limit damage to this vital organ. Here, we demonstrate that DENV NS3 protein interacts with GCKR, the negative regulator of the liver-specific hexokinase GCK and promotes glycolysis. Enhanced GCK expression and glycolytic activity correlates with an increase in DENV viral replication. By using in vitro and ex vivo models, we also established that inhibition of NAD(H) metabolism, which dampens cellular glycolysis, inhibits DENV replication. These findings provide a better

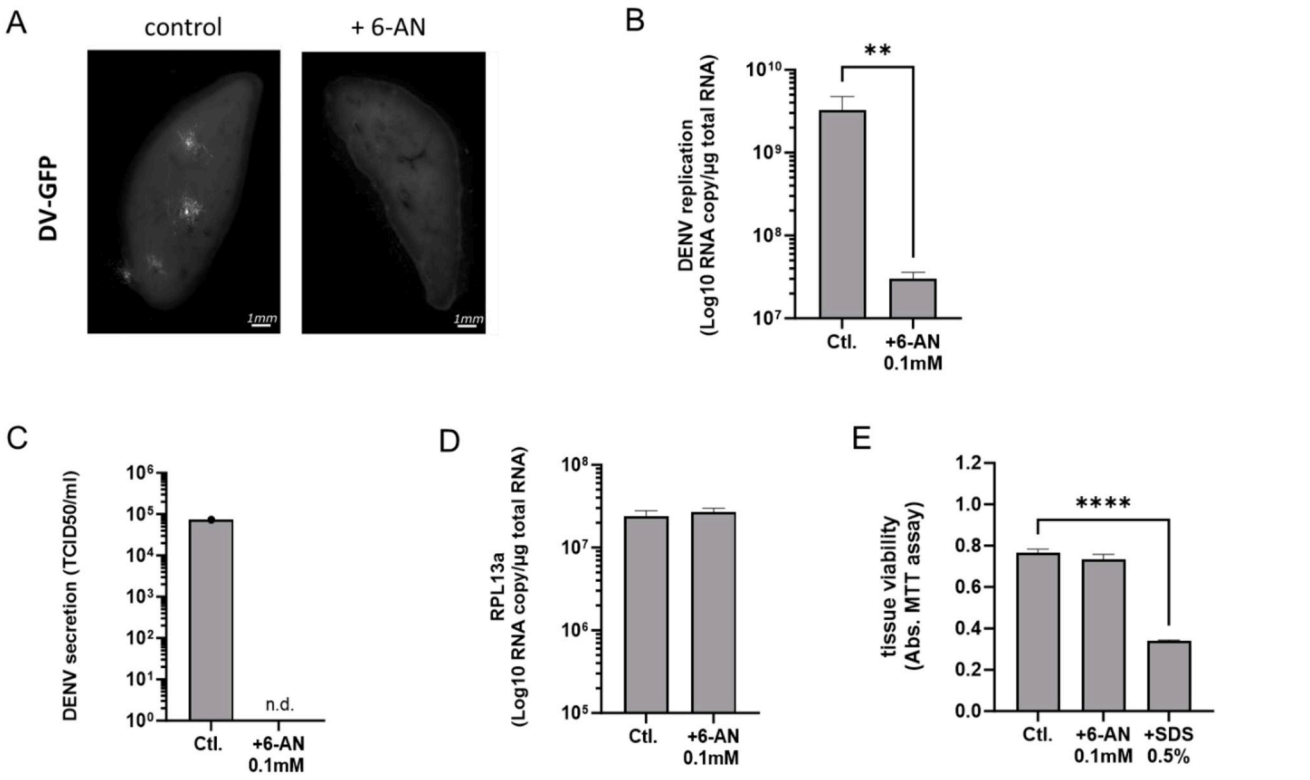

Fig. 8. 6-AN inhibits DENV infection in hamster OLiCs. OLiCs prepared as described in material and methods were infected with 10^3 PFU of DENV-GFP and treated or not with 6-AN at the concentration of 100 µM in the subnatant culture medium for 90 h. **A)** Observation of GFP foci by microscopy. Hamster OLiCs were imaged at day 4 post-infection using a Nikon Eclipse Ts2R epifluorescence microscope. Scalebar = 1 mm. **B)** DENV RNA were quantified in OLiC homogenates by specific qPCR and normalized to total cellular RNA extracted. Are presented quantification means ± SEM of 5 liver slices providing from 5 animals (n = 5, Mann-Whitney test, ** $p < 0.01$). **C)** Determination of DENV particle secretion in cell subnatants of the 5 liver slices. **D)** Quantification of ribosomal protein L13a (RPL13a) as an housekeeping gene in infected OLiCs at 90 h post-infection. **E)** After 90 h of treatment with 6-AN or SDS, determination of tissue metabolic activity by MTT assay was obtained by incubating slices with reagent for 2 h at 37 °C (n = 5, ANOVA, **** $p < 0.0001$).

understanding of molecular mechanisms by which DENV hijacks hepatocyte metabolism, and pave the way for host-directed therapies controlling DENV replication in the liver.

Only few studies have already analyzed the consequences of DENV infection on the metabolism of hepatocyte cells. A seminal work by El-Bacha et al. showed that in the HepG2 cell line, DENV infection induces a metabolic stress associated with mitochondrial dysfunction (El-Bacha et al., 2007). Following infection, intracellular ATP level collapses, highlighting the energy requirements and consumption associated with viral replication. Heaton et al. demonstrated in Huh7.5 cells (derived from Huh7 cells) that the viral protein NS3 recruits the cellular enzyme FASN at the replication site, thereby increasing intracellular lipid biosynthesis (Heaton et al., 2010). Fernandes-Siqueira et al. subsequently demonstrated that DENV replication in Huh7 cells increases glucose metabolism, and this plays an anaplerotic role in the oxidation of endogenous fatty acids (Fernandes-Siqueira et al., 2018). Our results, obtained in Huh7 cells engineered to re-express GCK alike normal hepatocyte, unravel a new molecular mechanism used by DENV to interfere with hepatocyte metabolism. Indeed, we showed that NS3 interacts with GCKR and increases glycolysis. One of the consequences of NS3 interaction with GCKR could be to prevent GCKR interaction with GCK due to steric hindrance. To investigate this hypothesis, we have carried out molecular docking simulation to build a three-dimensional model of the complex formed between NS3 and GCKR. We used the ClusPro server to dock NS3 onto GCKR as previously described using default parameters (Desta et al., 2020; Vajda et al., 2017; Kozakov et al., 2013, 2017). The obtained model of GCKR-NS3 complex (Supplementary Fig. 5A) was compared to the published 3D structure of the GCKR-GCK complex (PDB code 4LC9 and Supplementary Fig. 5B). The superimposition of the two complexes on the GCKR backbone revealed steric interference between GCK and NS3. Indeed, the site of NS3 interaction on GCKR is close to the site of interaction with GCK, as revealed by the tangle of NS3 and GCK if we try to make them both interact with GCKR (Supplementary Fig. 5C). It suggests that NS3 may interfere with GCKR capacity to bind and to inhibit GCK activity, thus explaining why NS3 expression increases glycolysis in Huh7-*GCK*$^+$/*HK2*$^-$ cells (Fig. 1B). This hypothesis is also in agreement with the increased replication observed when GCK was progressively overexpressed during viral replication (Fig. 4A). Overexpression of GCK, leads to higher quantity of free GCK that enhances cellular glycolytic activity, and thereby amplifying viral replication. Taken together, these observations suggest that it is the relative proportion of free GCK that could modulate viral replication. NS3, by modulating the availability of GCKR to interact with GCK, could therefore indirectly increase free GCK and thus boost its activity and, consequently, the viral replication that depends on it.

This interaction is of importance in hepatocytes since GCKR inhibitory activity on glycolysis is intimately linked to the expression of the liver-specific hexokinase GCK. Accordingly, GCKR overexpression or its enhanced interaction with GCK inhibits viral replication (Fig. 5). This further argues for DENV dependence on glycolysis in hepatocytes and NS3 interaction with GCKR appears to be specifically useful in the liver for controlling this essential pathway for viral replication. Interestingly, NS3 was previously described as a direct interactor of GAPDH, another glycolytic enzyme, reducing its activity (Silva et al., 2019). However, our results indicate that NS3 as well as DENV subgenomic replicon expression in hepatoma cells expressing GCK both result in enhanced activity of the glycolysis pathway, supporting the viral need of glucose metabolism (Fig. 1). Thus, NS3 protein may be able to modulate the

carbon flow in glycolysis in a complex manner, by interfering directly with glycolytic enzymes such as GAPDH or indirectly as a decoy for modulators of glycolysis such as GCKR. This multiple interference of the virus with glycolysis should enable adaptation to the infected host cell to maintain a high level of glycolysis. Finally, it highlights the capacity of DENV to enhance glycolysis in a multiple approach, according to metabolic specificity of the cell type and potentially whether certain isoenzymes such as hexokinases are expressed or not. Our observations also complement previous work showing that NS3 activates fatty acid biosynthesis in hepatocytes (Heaton et al., 2010). Indeed, the activation of glycolysis by DENV NS3 protein, is increasing the production of pyruvate that can fuel downstream metabolic pathways, such as TCA cycle and lipid biosynthesis. Altogether, this could contribute to the induction of transient steatosis as already reported in some patients.

Another major observation of our study is that inhibition of the cell's glycolytic capacity by down-regulation of NAD(H) metabolism strongly inhibits DENV replication both in vitro and ex vivo. We demonstrated the importance of NAD(H) metabolism in maintaining a high level of glucose metabolism and ATP synthesis to support viral replication (Figs. 6 and 7). Moreover, chemical inhibition of NAD(H) biosynthesis both in HCC cell lines and in liver slices inhibits viral replication (Figs. 6 and 8). Altogether, these observations highlight the importance of the intracellular pool of NAD(H) coenzyme to sustain the glycolytic flux induced during infection. As previously reported for Hepatitis B (Ren et al., 2019) and Zika (Sahoo et al., 2023) viruses, we observed that 6-AN was a potent inhibitor of DENV replication. However, the inhibitory effect of 6-AN on viral replication was not due to the inhibition of ribose-5-phosphate synthesis as suspected, but to its inhibitory effect on global NAD(H) metabolism. Indeed, we observed that 6-AN reduced the amount of intracellular NAD^+ and that viral replication was restored by the addition of NAM riboside, the precursor of NAD(H) synthesis by the salvage pathway. This could be linked to reduced glucose consumption and intracellular amounts of ATP upon 6-AN treatment that is restored by addition of NAM riboside. A similar mechanism was described for Zika virus replication (Sahoo et al., 2023), however according to our knowledge, this report shows for the first time DENV inhibition by 6-AN. Furthermore, this was established in Huh7-$GCK^+/HK2^-$ cells and ex-vivo in hamster liver slices (OLiCs). This latter model consists of slices of liver tissue obtained by cutting of the organ from animals immediately after sacrifice. Slices are cultured and infected at the air/liquid interface on microporous membranes as previously described for other organs and with other viruses (Ferren et al., 2021; Shyfrin et al., 2022). Organotypic cultures allow the tissue physiological structure and organization to be preserved with all cell types and the intercellular connections within the tissue. This culture system is therefore able to bridge the gap between the simplicity of cell cultures and the excessive complexity of an animal model. It enables infection of liver cells in a 3D culture system characteristic of the tissue and maintenance of the low proliferation of these cells in their native context. Under these conditions, we observed a 2 $\log_{10}$ inhibition of viral replication with 6-AN and total inhibition of infectious particle secretion with no appreciable effect on cell viability (Fig. 8 and Supplementary Fig. 4). Indeed, in the liver NAD(H) metabolism is central in both catabolic and anabolic pathways such as glucogenesis, glycogenesis or lipogenesis. The antimetabolite 6-AN has been used for decades in preclinical trial in combination with other chemicals to increase the effectiveness of treatment in many cancers, including liver cancer (Dietrich et al., 1968; Dewey and Hawes, 1963). Recently, in the light of a better-provided rational, 6-AN has been re-purposed in preclinical studies because of its ability to inhibit PPP (Li et al., 2013; Kaushik et al., 2021; Arbe et al., 2020). Induction of reactive oxygen species (ROS)-mediated apoptosis by ER stress in lung cancer cells was involved (Kaushik et al., 2021). Our study strongly suggests that targeting NAD metabolism to inhibit glycolysis, and thus the capacity of cells to replicate the virus, could be an efficient therapeutic approach to control dengue infection in liver. This is especially relevant as hepatocytes have the intrinsic capacity to increase glycolysis when blood glucose concentration rises which could allow increased viral replication.

The use of therapeutic molecules targeting host rather than viral proteins is a promising strategy, since it limits the risk of developing resistance due to a higher genetic barrier, and has a broader potential of action since it can render the host refractory to infection. Identification of the interaction between NS3 and GCKR, that is regulating glycolysis activity in the liver, should therefore pave the way to develop host metabolism directed strategies to limit hepatic infection and associated complications.

Funding

This research was funded by the Fondation pour la Recherche Médicale (FRM), grant number DEQ20160334893 to V.L. and by the Agence Nationale de Recherches sur le Sida et les hépatites virales (ANRS|Maladies infectieuses émergentes), grant numbers ASA21007-CRA, and ECTZ244976 to O.D.

Ethics approval

Research involving animals was performed according to French ethical committee (CECCAPP) regulations (accreditation CECCAPP_ENS_2014_034).

CRediT authorship contribution statement

Eva Ogire: Investigation. **Laure Perrin-Cocon:** Writing – review & editing, Investigation, Conceptualization. **Marianne Figl:** Investigation. **Cindy Kundlacz:** Investigation. **Clémence Jacquemin:** Investigation. **Sophie Hubert:** Investigation. **Anne Aublin-Gex:** Investigation. **Johan Toesca:** Investigation. **Christophe Ramière:** Investigation. **Pierre-Olivier Vidalain:** Writing – review & editing, Methodology, Conceptualization. **Cyrille Mathieu:** Writing – review & editing, Methodology, Conceptualization. **Vincent Lotteau:** Writing – review & editing, Methodology, Conceptualization. **Olivier Diaz:** Writing – review & editing, Writing – original draft, Supervision, Methodology, Investigation, Conceptualization.

Declaration of competing interest

The authors declare that they have no known competing financial interests or personal relationships that could have appeared to influence the work reported in this paper.

Data availability

Data will be made available on request.

5. Acknowledgments

We acknowledge the contribution of SFR Biosciences (UMS3444/CNRS, US8/INSERM, ENS de Lyon, UCBL) facilities: AniRA-PBES platform for animal housing, AniRA – Laboratoire L3 platform for infection experiments and LYMICPLATIM platform for microscopy. We thank Ralf Bartenschlager for providing plasmids containing cDNA for replicons.

Appendix A. Supplementary data

Supplementary data to this article can be found online at https://doi.org/10.1016/j.antiviral.2024.105939.

References

Allonso, D., Andrade, I.S., Conde, J.N., Coelho, D.R., Rocha, D.C.P., da Silva, M.L., Ventura, G.T., Silva, E.M., Mohana-Borges, R., 2015. Dengue virus NS1 protein

modulates cellular energy metabolism by increasing glyceraldehyde-3-phosphate dehydrogenase activity. J. Virol. 89, 11871–11883. https://doi.org/10.1128/JVI.01342-15.
Arbe, M.F., Agnetti, L., Breininger, E., Glikin, G.C., Finocchiaro, L.M.E., Villaverde, M.S., 2020. Glucose 6-phosphate dehydrogenase inhibition sensitizes melanoma cells to metformin treatment. Transl Oncol 13, 100842. https://doi.org/10.1016/j.tranon.2020.100842.
Aye, K.S., Charngkaew, K., Win, N., Wai, K.Z., Moe, K., Punyadee, N., Thiemmeca, S., Suttitheptumrong, A., Sukpanichnant, S., Prida, M., Halstead, S.B., 2014. Pathologic highlights of dengue hemorrhagic fever in 13 autopsy cases from Myanmar. Hum. Pathol. 45, 1221–1233. https://doi.org/10.1016/j.humpath.2014.01.022.
Beck, T., Miller, B.G., 2013. Structural basis for regulation of human glucokinase by glucokinase regulatory protein. Biochemistry 52, 6232–6239. https://doi.org/10.1021/bi400838t.
Chatel-Chaix, L., Cortese, M., Romero-Brey, I., Bender, S., Neufeldt, C.J., Fischl, W., Scaturro, P., Schieber, N., Schwab, Y., Fischer, B., Ruggieri, A., Bartenschlager, R., 2016. Dengue virus perturbs mitochondrial morphodynamics to dampen innate immune responses. Cell Host Microbe 20, 342–356. https://doi.org/10.1016/j.chom.2016.07.008.
Choi, J.M., Seo, M.-H., Kyeong, H.-H., Kim, E., Kim, H.-S., 2013. Molecular basis for the role of glucokinase regulatory protein as the allosteric switch for glucokinase. Proc. Natl. Acad. Sci. USA 110, 10171–10176. https://doi.org/10.1073/pnas.1300457110.
Choi, S.G., Olivet, J., Cassonnet, P., Vidalain, P.-O., Luck, K., Lambourne, L., Spirohn, K., Lemmens, I., Dos Santos, M., Demeret, C., Jones, L., Rangarajan, S., Bian, W., Coutant, E.P., Janin, Y.L., van der Werf, S., Trepte, P., Wanker, E.E., De Las Rivas, J., Tavernier, J., Twizere, J.-C., Hao, T., Hill, D.E., Vidal, M., Calderwood, M.A., Jacob, Y., 2019. Maximizing binary interactome mapping with a minimal number of assays. Nat. Commun. 10 https://doi.org/10.1038/s41467-019-11809-2.
Coutant, E.P., Goyard, S., Hervin, V., Gagnot, G., Baatallah, R., Jacob, Y., Rose, T., Janin, Y.L., 2019. Gram-scale synthesis of luciferins derived from coelenterazine and original insights into their bioluminescence properties. Org. Biomol. Chem. 17, 3709–3713. https://doi.org/10.1039/c9ob00459a.
de Chassey, B., Navratil, V., Tafforeau, L., Hiet, M.S., Aublin-Gex, A., Agaugué, S., Meiffren, G., Pradezynski, F., Faria, B.F., Chantier, T., Le Breton, M., Pellet, J., Davoust, N., Mangeot, P.E., Chaboud, A., Penin, F., Jacob, Y., Vidalain, P.O., Vidal, M., André, P., Rabourdin-Combe, C., Lotteau, V., 2008. Hepatitis C virus infection protein network. Mol. Syst. Biol. 4, 230. https://doi.org/10.1038/msb.2008.66.
Desta, I.T., Porter, K.A., Xia, B., Kozakov, D., Vajda, S., 2020. Performance and its limits in rigid body protein-protein docking. Structure 28, 1071–1081.e3. https://doi.org/10.1016/j.str.2020.06.006.
Dewey, D.L., Hawes, C., 1963. 6-AMINONICOTINAMIDE and the radiosensitivity of human liver cells in culture. Nature 200, 1176–1178. https://doi.org/10.1038/2001176a0.
Diamond, D.L., Syder, A.J., Jacobs, J.M., Sorensen, C.M., Walters, K.-A., Proll, S.C., McDermott, J.E., Gritsenko, M.A., Zhang, Q., Zhao, R., Metz, T.O., Camp, D.G., Waters, K.M., Smith, R.D., Rice, C.M., Katze, M.G., 2010. Temporal proteome and lipidome profiles reveal hepatitis C virus-associated reprogramming of hepatocellular metabolism and bioenergetics. PLoS Pathog. 6, e1000719 https://doi.org/10.1371/journal.ppat.1000719.
Diaz, O., Cubero, M., Trabaud, M.A., Quer, J., Icard, V., Esteban, J.I., Lotteau, V., André, P., 2008. Transmission of low-density hepatitis C viral particles during sexually transmitted acute resolving infection. J. Med. Virol. 80, 242–246. https://doi.org/10.1002/jmv.21037.
Diaz, O., Vidalain, P.-O., Ramière, C., Lotteau, V., Perrin-Cocon, L., 2022. What role for cellular metabolism in the control of hepatitis viruses? Front. Immunol. 13.
Dietrich, L.S., Muniz, O., Farinas, B., Franklin, L., 1968. 6-aminonicotinamide-14C utilization by the 755 tumor and host liver tissue. Cancer Res. 28, 1652–1654.
Dubuisson, J., Cosset, F.-L., 2014. Virology and cell biology of the hepatitis C virus life cycle – an update. J. Hepatol. 61, S3–S13. https://doi.org/10.1016/j.jhep.2014.06.031.
El-Bacha, T., Midlej, V., Pereira, da Silva AP., Silva da Costa, L., Benchimol, M., Galina, A., Da Poian, A.T., 2007. Mitochondrial and bioenergetic dysfunction in human hepatic cells infected with dengue 2 virus. Biochim. Biophys. Acta (BBA) - Mol. Basis Dis. 1772, 1158–1166. https://doi.org/10.1016/j.bbadis.2007.08.003.
Erken, R., Andre, P., Roy, E., Kootstra, N., Barzic, N., Girma, H., Laveille, C., Radreau-Pierini, P., Darteil, R., Vondercher, J., Scalfaro, P., Tangkijvanich, P., Flisiak, R., Reesink, H., 2021. Farnesoid X receptor agonist for the treatment of chronic hepatitis B: a safety study. J. Viral Hepat. 28, 1690–1698. https://doi.org/10.1111/jvh.13608.
Fernandes-Siqueira, L.O., Zeidler, J.D., Sousa, B.G., Ferreira, T., Poian, A.T.D., 2018. Anaplerotic role of glucose in the oxidation of endogenous fatty acids during dengue virus infection. mSphere 3, e00458. https://doi.org/10.1128/mSphere.00458-17, 17.
Ferren, M., Favède, V., Decimo, D., Iampietro, M., Lieberman, N.A.P., Weickert, J.-L., Pelissier, R., Mazelier, M., Terrier, O., Moscona, A., Porotto, M., Greninger, A.L., Messaddeq, N., Horvat, B., Mathieu, C., 2021. Hamster organotypic modeling of SARS-CoV-2 lung and brainstem infection. Nat. Commun. 12, 5809. https://doi.org/10.1038/s41467-021-26096-z.
Fischl, W., Bartenschlager, R., 2013. High-throughput screening using dengue virus reporter genomes. In: Gong, E.Y. (Ed.), Antiviral Methods and Protocols. Humana Press, Totowa, NJ, pp. 205–219.
Fontaine, K.A., Sanchez, E.L., Camarda, R., Lagunoff, M., 2014. Dengue virus induces and requires glycolysis for optimal replication. J. Virol. https://doi.org/10.1128/JVI.02309-14.
Giraud, E., del Val, C.O., Caillet-Saguy, C., Zehrouni, N., Khou, C., Caillet, J., Jacob, Y., Pardigon, N., Wolff, N., 2021. Role of PDZ-binding motif from West Nile virus NS5 protein on viral replication. Sci. Rep. 11, 3266. https://doi.org/10.1038/s41598-021-82751-x.
Girdhar, K., Powis, A., Raisingani, A., Chrudinová, M., Huang, R., Tran, T., Sevgi, K., Dogus Dogru, Y., Altindis, E., 2021. Viruses and metabolism: the effects of viral infections and viral insulins on host metabolism. Annu Rev Virol 8, 373–391. https://doi.org/10.1146/annurev-virology-091919-102416.
Hafirassou, M.L., Meertens, L., Umaña-Diaz, C., Labeau, A., Dejarnac, O., Bonnet-Madin, L., Kümmerer, B.M., Delaugerre, C., Roingeard, P., Vidalain, P.-O., Amara, A., 2017. A global interactome map of the dengue virus NS1 identifies virus restriction and dependency host factors. Cell Rep. 21, 3900–3913. https://doi.org/10.1016/j.celrep.2017.11.094.
Heaton, N.S., Perera, R., Berger, K.L., Khadka, S., LaCount, D.J., Kuhn, R.J., Randall, G., 2010. Dengue virus nonstructural protein 3 redistributes fatty acid synthase to sites of viral replication and increases cellular fatty acid synthesis. Proc. Natl. Acad. Sci. USA 107, 17345–17350. https://doi.org/10.1073/pnas.1010811107.
Jordan, T.X., Randall, G., 2016. Flavivirus modulation of cellular metabolism. Curr Opin Virol 19, 7–10. https://doi.org/10.1016/j.coviro.2016.05.007.
Jordan, T.X., Randall, G., 2017. Dengue virus activates the AMP kinase-mTOR Axis to stimulate a proviral lipophagy. J. Virol. 91 https://doi.org/10.1128/JVI.02020-16.
Kao, Y.-T., Chang, B.-L., Liang, J.-J., Tsai, H.-J., Lee, Y.-L., Lin, R.-J., Lin, Y.-L., 2015. Japanese encephalitis virus nonstructural protein NS5 interacts with mitochondrial trifunctional protein and impairs fatty acid β-oxidation. PLoS Pathog. 11, e1004750 https://doi.org/10.1371/journal.ppat.1004750.
Kaushik, N., Kaushik, N.K., Choi, E.H., Kim, J.H., 2021. Blockade of cellular energy metabolism through 6-aminonicotinamide reduces proliferation of non-small lung cancer cells by inducing endoplasmic reticulum stress. Biology 10, 1088. https://doi.org/10.3390/biology10111088.
Kozakov, D., Beglov, D., Bohnuud, T., Mottarella, S.E., Xia, B., Hall, D.R., Vajda, S., 2013. How good is automated protein docking? Proteins 81, 2159–2166. https://doi.org/10.1002/prot.24403.
Kozakov, D., Hall, D.R., Xia, B., Porter, K.A., Padhorny, D., Yueh, C., Beglov, D., Vajda, S., 2017. The ClusPro web server for protein–protein docking. Nat. Protoc. 12, 255–278. https://doi.org/10.1038/nprot.2016.169.
Lamesch, P., Li, N., Milstein, S., Fan, C., Hao, T., Szabo, G., Hu, Z., Venkatesan, K., Bethel, G., Martin, P., Rogers, J., Lawlor, S., McLaren, S., Dricot, A., Borick, H., Cusick, M.E., Vandenhaute, J., Dunham, I., Hill, D.E., Vidal, M., 2007. hORFeome v3.1: a resource of human open reading frames representing over 10,000 human genes. Genomics 89, 307–315. https://doi.org/10.1016/j.ygeno.2006.11.012.
Lee, Y.-R., Wu, S.-Y., Chen, R.-Y., Lin, Y.-S., Yeh, T.-M., Liu, H.-S., 2020. Regulation of autophagy, glucose uptake, and glycolysis under dengue virus infection. Kaohsiung J. Med. Sci. 36, 911–919. https://doi.org/10.1002/kjm2.12271.
Leowattana, W., Leowattana, T., 2021. Dengue hemorrhagic fever and the liver. World J. Hepatol. 13, 1968–1976. https://doi.org/10.4254/wjh.v13.i12.1968.
Li, X., Fang, P., Mai, J., Choi, E.T., Wang, H., Yang, X., 2013. Targeting mitochondrial reactive oxygen species as novel therapy for inflammatory diseases and cancers. J. Hematol. Oncol. 6, 19. https://doi.org/10.1186/1756-8722-6-19.
Lindenbach, B.D., Evans, M.J., Syder, A.J., Wölk, B., Tellinghuisen, T.L., Liu, C.C., Maruyama, T., Hynes, R.O., Burton, D.R., McKeating, J.A., Rice, C.M., 2005. Complete replication of hepatitis C virus in cell culture. Science 309, 623–626. https://doi.org/10.1126/science.1114016.
Martín-Acebes, M.A., Merino-Ramos, T., Blázquez, A.-B., Casas, J., Escribano-Romero, E., Sobrino, F., Saiz, J.-C., 2014. The composition of West Nile virus lipid envelope unveils a role of sphingolipid metabolism in flavivirus biogenesis. J. Virol. 88, 12041–12054. https://doi.org/10.1128/JVI.02061-14.
Martín-Acebes, M.A., Jiménez de Oya, N., Saiz, J.-C., 2019. Lipid metabolism as a source of druggable targets for antiviral discovery against Zika and other flaviviruses. Pharmaceuticals 12. https://doi.org/10.3390/ph12020097.
Mayer, K.A., Stöckl, J., Zlabinger, G.J., Gualdoni, G.A., 2019. Hijacking the supplies: metabolism as a novel facet of virus-host interaction. Front. Immunol. 10, 1533. https://doi.org/10.3389/fimmu.2019.01533.
Mrzljak, A., Tabain, I., Premac, H., Bogdanic, M., Barbic, L., Savic, V., Stevanovic, V., Jelic, A., Mikulic, D., Vilibic-Cavlek, T., 2019. The role of emerging and neglected viruses in the etiology of hepatitis. Curr. Infect. Dis. Rep. 21, 51. https://doi.org/10.1007/s11908-019-0709-2.
Pauly, D.F., Pepine, C.J., 2000. D-ribose as a supplement for cardiac energy metabolism. J. Cardiovasc. Pharmacol. Therapeut. 5, 249–258. https://doi.org/10.1054/JCPT.2000.18011.
Perrin-Cocon, L., Diaz, O., Jacquemin, C., Barthel, V., Ogire, E., Ramière, C., André, P., Lotteau, V., Vidalain, P.-O., 2020. The current landscape of coronavirus-host protein-protein interactions. J. Transl. Med. 18, 319. https://doi.org/10.1186/s12967-020-02480-z.
Perrin-Cocon, L., Vidalain, P.-O., Jacquemin, C., Aublin-Gex, A., Olmstead, K., Panthu, B., Rautureau, G.J.P., André, P., Nyczka, P., Hütt, M.-T., Amoedo, N., Rossignol, R., Filipp, F.V., Lotteau, V., Diaz, O., 2021. A hexokinase isoenzyme switch in human liver cancer cells promotes lipogenesis and enhances innate immunity. Commun. Biol. 4, 1–15. https://doi.org/10.1038/s42003-021-01749-3.
Perrin-Cocon, L., Kundlacz, C., Jacquemin, C., Hanoulle, X., Aublin-Gex, A., Figl, M., Manteca, J., André, P., Vidalain, P.-O., Lotteau, V., Diaz, O., 2022. Domain 2 of hepatitis C virus protein NS5A activates glucokinase and induces lipogenesis in hepatocytes. Int. J. Mol. Sci. 23, 919. https://doi.org/10.3390/ijms23020919.
Piver, E., Boyer, A., Gaillard, J., Bull, A., Beaumont, E., Roingeard, P., Meunier, J.-C., 2017. Ultrastructural organisation of HCV from the bloodstream of infected patients revealed by electron microscopy after specific immunocapture. Gut 66, 1487–1495. https://doi.org/10.1136/gutjnl-2016-311726.

Ramière, C., Rodriguez, J., Enache, L.S., Lotteau, V., André, P., Diaz, O., 2014. Activity of hexokinase is increased by its interaction with hepatitis C virus protein NS5A. J. Virol. 88, 3246–3254. https://doi.org/10.1128/JVI.02862-13.

Ren, F., Yang, X., Hu, Z.-W., Wong, V.K.W., Xu, H.-Y., Ren, J.-H., Zhong, S., Jia, X.-J., Jiang, H., Hu, J.-L., Cai, X.-F., Zhang, W.-L., Yao, F.-L., Yu, H.-B., Cheng, S.-T., Zhou, H.-Z., Huang, A.-L., Law, B.Y.K., Chen, J., 2019. Niacin analogue, 6-Amino-nicotinamide, a novel inhibitor of hepatitis B virus replication and HBsAg production. EBioMedicine 49, 232–246. https://doi.org/10.1016/j.ebiom.2019.10.022.

Sahoo, B.R., Crook, A.A., Pattnaik, A., Torres-Gerena, A.D., Khalimonchuk, O., Powers, R., Franco, R., Pattnaik, A.K., 2023. Redox regulation and metabolic dependency of Zika virus replication: inhibition by nrf2-antioxidant response and NAD(H) antimetabolites. J. Virol. 97, e01363 https://doi.org/10.1128/jvi.01363-22, 22.

Sanchez, E.L., Lagunoff, M., 2015. Viral activation of cellular metabolism. Virology 479–480, 609–618. https://doi.org/10.1016/j.virol.2015.02.038.

Scholtes, C., Diaz, O., Icard, V., Kaul, A., Bartenschlager, R., Lotteau, V., André, P., 2008. Enhancement of genotype 1 hepatitis C virus replication by bile acids through FXR. J. Hepatol. 48, 192–199. https://doi.org/10.1016/j.jhep.2007.09.015.

Scholtes, C., Ramière, C., Rainteau, D., Perrin-Cocon, L., Wolf, C., Humbert, L., Carreras, M., Guironnet-Paquet, A., Zoulim, F., Bartenschlager, R., Lotteau, V., André, P., Diaz, O., 2012. High plasma level of nucleocapsid-free envelope glycoprotein-positive lipoproteins in hepatitis C patients. Hepatology 56, 39–48. https://doi.org/10.1002/hep.25628.

Shimotohno, K., 2021. HCV assembly and egress via modifications in host lipid metabolic systems. Cold Spring Harb Perspect Med 11, a036814. https://doi.org/10.1101/cshperspect.a036814.

Shyfrin, S.R., Ferren, M., Perrin-Cocon, L., Espi, M., Charmetant, X., Brailly, M., Decimo, D., Iampietro, M., Canus, L., Horvat, B., Lotteau, V., Vidalain, P.-O., Thaunat, O., Mathieu, C., 2022. Hamster organotypic kidney culture model of early-stage SARS-CoV-2 infection highlights a two-step renal susceptibility. J. Tissue Eng. 13, 20417314221122130 https://doi.org/10.1177/20417314221122130.

Silva, E.M., Conde, J.N., Allonso, D., Ventura, G.T., Coelho, D.R., Carneiro, P.H., Silva, M.L., Paes, M.V., Rabelo, K., Weissmuller, G., Bisch, P.M., Mohana-Borges, R., 2019. Dengue virus nonstructural 3 protein interacts directly with human glyceraldehyde-3-phosphate dehydrogenase (GAPDH) and reduces its glycolytic activity. Sci. Rep. 9, 1–19. https://doi.org/10.1038/s41598-019-39157-7.

Suksanpaisan, L., Cabrera-Hernandez, A., Smith, D.R., 2007. Infection of human primary hepatocytes with dengue virus serotype 2. J. Med. Virol. 79, 300–307. https://doi.org/10.1002/jmv.20798.

Thaker, S.K., Ch'ng, J., Christofk, H.R., 2019. Viral hijacking of cellular metabolism. BMC Biol. 17, 59. https://doi.org/10.1186/s12915-019-0678-9.

Tseng, H., Gage, J.A., Shen, T., Haisler, W.L., Neeley, S.K., Shiao, S., Chen, J., Desai, P.K., Liao, A., Hebel, C., Raphael, R.M., Becker, J.L., Souza, G.R., 2015. A spheroid toxicity assay using magnetic 3D bioprinting and real-time mobile device-based imaging. Sci. Rep. 5, 13987 https://doi.org/10.1038/srep13987.

Vajda, S., Yueh, C., Beglov, D., Bohnuud, T., Mottarella, S.E., Xia, B., Hall, D.R., Kozakov, D., 2017. New additions to the ClusPro server motivated by CAPRI. Proteins 85, 435–444. https://doi.org/10.1002/prot.25219.

Welch, J., Wallace, J., Lansley, A.B., Roper, C., 2021. Evaluation of the toxicity of sodium dodecyl sulphate (SDS) in the MucilAir™ human airway model in vitro. Regul. Toxicol. Pharmacol. 125, 105022 https://doi.org/10.1016/j.yrtph.2021.105022.

Welsch, J.C., Lionnet, C., Terzian, C., Horvat, B., Gerlier, D., Mathieu, C., 2017. Organotypic brain cultures: a framework for studying CNS infection by neurotropic viruses and screening antiviral drugs. Bio Protoc 7, e2605. https://doi.org/10.21769/BioProtoc.2605.